

DOI: 10.1070/QEL16235

Generation of frequency-tunable pulsed terahertz radiation by a Cr:forsterite laser system with an acoustooptical control of the pulse temporal profile

A.V. Ovchinnikov, O.V. Chefonov, V.Ya. Molchanov, K.B. Yushkov, C. Vicario, C. Hauri

Abstract. **We report the experimental results on generating pulsed terahertz (THz) radiation, frequency-tunable within the range 0.5–2 THz. The THz pulse generation was implemented using the method of optical rectification of femtosecond laser pulses in the nonlinear organic crystal OH1. The frequency tuning of the THz radiation was provided by adaptive phase–amplitude modulation of the pump pulses from the Cr:forsterite laser system with a radiation wavelength of 1230 nm using the acoustooptical dispersion delay line.**

Keywords: *femtosecond laser pulse, optical rectification, terahertz radiation, acoustooptical dispersion delay line.*

1. Introduction

Recent progress in the field of generating terahertz (THz) radiation offered new possibilities for constructing pulsed sources with a high pulse energy and electric field strength [1–6]. As a rule, such sources possess broad spectra, overlapping the frequency range of a few THz, while for many practical applications it is desirable to use a narrow-band pulse of THz radiation, tunable within a certain frequency range. For example, using such a pulse one can selectively excite the modes close to resonance with the THz source frequency without affecting the adjacent modes, search for new frequency components arising in nonlinear THz processes, etc. However, until now there have been no efficient methods of adaptive formation of THz pulses with the specified spectral and temporal shape.

To generate subpicosecond pulses of high-energy THz radiation the methods of nonlinear interaction of pump femtosecond laser pulses (FLPs) with different nonlinear crystals are used. Nahata et al. [7] obtained THz pulses with a wide spectrum by pumping the inorganic nonlinear ZnTe crystal with 800-nm femtosecond laser pulses. The mean power of radiation attained 150 μW at a pulse repetition rate of 100 Hz [8], but the mean efficiency of converting the laser pulse energy into the THz pulse energy (conversion efficiency) in the crystal did not exceed 10^{-5}. Efficient generation of such pulses using the method of laser pulse optical rectification with the radiation wavelength 1.03 μm in the $LiNbO_3$ crystal using the optical scheme with oblique wave front to provide phase matching was observed in Ref. [9]. The pulse energy achieved 100 nJ in the spectral range up to 2.5 THz, and the conversion efficiency amounted to 2.5×10^{-4}, which is by an order of magnitude greater than that in ZnTe or GaP crystals. A considerable increase in the efficiency of THz generation in the $LiNbO_3$ crystal was achieved under cryogenic cooling [3]. The conversion efficiency was greater by two orders of magnitude and achieved 3.8% ± 0.4%. To obtain such a conversion efficiency, the high pump energy density is required with the optimised pulse duration and spectral width.

Relatively new-developed organic nonlinear electrooptic crystals for generating the THz pulses using the method of optical rectification allow one to receive the comparable conversion efficiency in a simpler scheme of collinear matching (as in ZnTe and GaP crystals) and at lower energies of the laser pump pulses [10]. The maximal THz pulse energy of 0.9 mJ with the conversion efficiency 3% was obtained using the optical rectification of a femtosecond laser pulse by a Cr:forsterite laser system in the nonlinear organic crystal DSTMS [11].

The broad emission spectrum of femtosecond lasers allows the generation of THz pulses with a narrow spectrum by mixing two chirped pulses, delayed with respect to each other in a nonlinear medium [12]. In Ref. [13] THz pulses with the energy of a few microjoules, frequency-tunable within the range 0.3–1.3 THz, were generated using the method of optical rectification in the $LiNbO_3$ crystal pumped with a multipeak optical pulse. The generation of THz pulses with a tunable centre frequency in the range 0.3–0.8 THz in the nonlinear organic crystal HMQ-TMS using the method of optical rectification of femtosecond laser pulses at the radiation wavelength 800 nm with a modified temporal shape of the pulse was studied in Ref. [14]. In the above papers, the pair of delayed identical pulses required to generate the frequency-tunable Hz radiation was provided using interferometers of various types.

One more rather simple method to generate a variable-frequency THz pulse is to use a femtosecond pump pulse with amplitude modulation in the transverse section of the beam. This method was used in Ref. [15], where for modulating the laser beam the authors used a shadow mask, formed by a periodic sequence of slits, transmitting laser radiation. The THz radiation frequency was determined by the period of the

A.V. Ovchinnikov, O.V. Chefonov Joint Institute for High Temperatures, Russian Academy of Sciences, ul. Izhorskaya 13, Bld. 2, 125412 Moscow, Russia;
e-mail: ovtch2006@yandex.ru, oleg.chefonov@gmail.com;
V.Ya. Molchanov, K.B. Yushkov National University of Science and Technology MISiS, Leninsky prosp. 4, 119049 Moscow, Russia;
C. Vicario, C. Hauri Paul Scherrer Institute, SwissFEL, 5232 Villigen PSI, Switzerland

Received 13 October 2016; revision received 10 November 2016
Kvantovaya Elektronika **46** (12) 1149–1153 (2016)
Translated by V.L. Derbov

shadow mask slits. The method based on using a phase mask [16] is an alternative to the shadow-mask method.

The generation of narrow-band THz pulses was also implemented by means of the programmable liquid-crystal modulator used to form the required temporal shape of the laser pump pulses [17]. Using the method of optical rectification of pulses from the femtosecond Ti:sapphire laser in the ZnTe crystal, the pulses with the centre frequency in the range 0.5–2 THz, the spectral width ~0.2 THz but very low (~10 fJ) pulse energy were generated.

The general drawback of all above methods for generating frequency-tunable THz radiation is the great (up to 50%) loss of energy of the pump FLP, which, in turn, reduces the output energy of the THz radiation.

The goal of the present paper is to demonstrate a new method of forming laser pulses with a prescribed temporal profile of intensity and the application of these pulses for generating frequency-tunable THz pulses. The method is based on the variation of the period of the amplitude–phase modulation of the femtosecond pump pulses by means of acoustooptical dispersion delay line (AODDL) with a complex-valued spectral transmission function [18–20]. The use of adaptive AODDL allows simultaneous and independent tuning of both the frequency and the spectral width of THz radiation. In the AODDL, the energy loss can be completely compensated for in the amplifier units, operating in the saturation regime. The generation of narrow-band frequency-tunable THz pulses was implemented using the method of optical rectification of chirped laser pulses from a high-power Cr:forsterite laser system in the nonlinear organic crystal OH1 [(2-(3-(4-Hydroxystyryl)-5,5-dimethylcyclohex-2-enylidene) malononitrile)]. The application of nonlinear organic crystals, as pointed out in Refs [11, 21], is caused by the high efficiency of conversion of the energy of a pump pulse generated by the Cr:forsterite laser system into the energy of the THz pulse.

2. Experimental setup

High-power FLPs were generated by the terawatt Cr:forsterite laser system [22], the front end of which had the electronically controlled AODDL. The experimental setup is schematically illustrated in Fig.1. The laser system was assembled according to the standard CPA-scheme of amplifying chirped pulses and comprised a master oscillator, a stretcher, a regenerative amplifier, three multipass amplifiers and a temporal compressor. The master oscillator formed the pulses with the energy 3 nJ, the duration 60 fs, and the spectral width 45 nm at the centre wavelength 1260 nm and the repetition rate 70 MHz. The AODDL was installed between the master oscillator and the stretcher and implemented the phase–amplitude modulation of the laser pulse spectrum, aimed to form the radiation with the required temporal profile at the output of the laser system. At the output of the laser system, the pulse energy achieved 40 mJ with the spectral width 25 nm at the radiation wavelength 1230 nm and the repetition rate 10 Hz.

The AODDL based on the monocrystalline paratellurite had the quasi-collinear interaction geometry and possessed a high spectral resolution [23, 24]. The length of the acoustooptical crystal was equal to 67 mm. The width of the AODDL instrument function at the wavelength 1260 nm amounted to 0.24 nm at the –3 dB level. Since the AODDL can implement both positive and negative dispersion, the zero value was chosen as the dispersions of the second and the third order equal in magnitude and opposite in sign to the material dispersion of the paratellurite crystal. Thus, in the absence of modulation, the FLP at the AODDL output remained transform limited. The AODDL formed two identical chirped pulses shifted in time by τ. The complex-valued transmission function in this case has the form

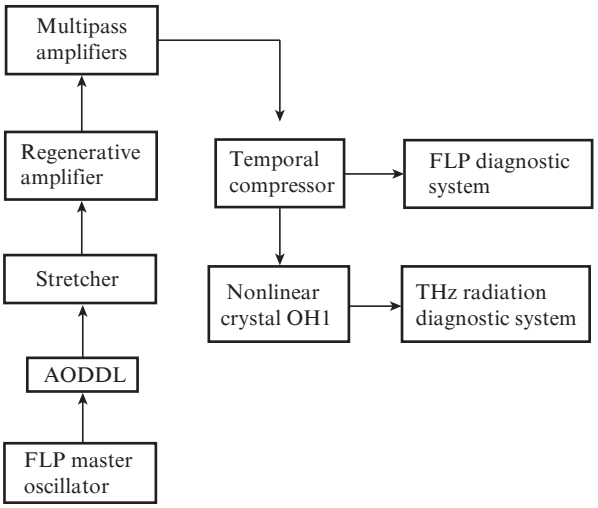

Figure 1. Schematic of the experimental setup (AODDL is the acoustooptical dispersion delay line).

$$H(\omega) = [1 + \exp(i\omega\tau)]\exp[iD_2(\omega - \omega_0)^2], \quad (1)$$

where D_2 is the second-order dispersion; ω_0 is the circular frequency of the radiation, corresponding to the centre wavelength of the spectrum. The duration of the chirped pulse T_1 is determined by the dispersion D_2 and the duration T_0 of the spectrally limited FLP, and if $D_2 \gg T_0^2$, then the following approximate relation is valid:

$$T_1 = \frac{|D_2|}{T_0}, \quad (2)$$

where T_0 and T_1 correspond to full durations of the envelopes of the corresponding pulses at the level $1/e^2$.

The first factor in expression (1) varies in magnitude, due to which the modulation of the output is observed, having the period

$$\Delta\lambda = \frac{\lambda^2}{2\pi c\tau}$$

(c is the velocity of light). In turn, this leads to the sinusoidal temporal modulation of the chirped pulses with the period proportional to D_2 and $\Delta\lambda$. Thus, the complex-valued transmission function of the AODDL (1) gives rise to the periodic modulation of the envelope of the output chirped pulses.

As a result of using this method of controlling the laser pulse spectrum, two pulses were generated at the output of the laser system with a controllable delay between them. The pulses were incident on the nonlinear organic crystal OH1 for optical rectification in the collinear geometry under the phase-matching conditions. Figure 2 presents the measured second-order autocorrelation functions for two pulses with the relative delay τ = 1.1 ps. The temporal profile of the laser pulse

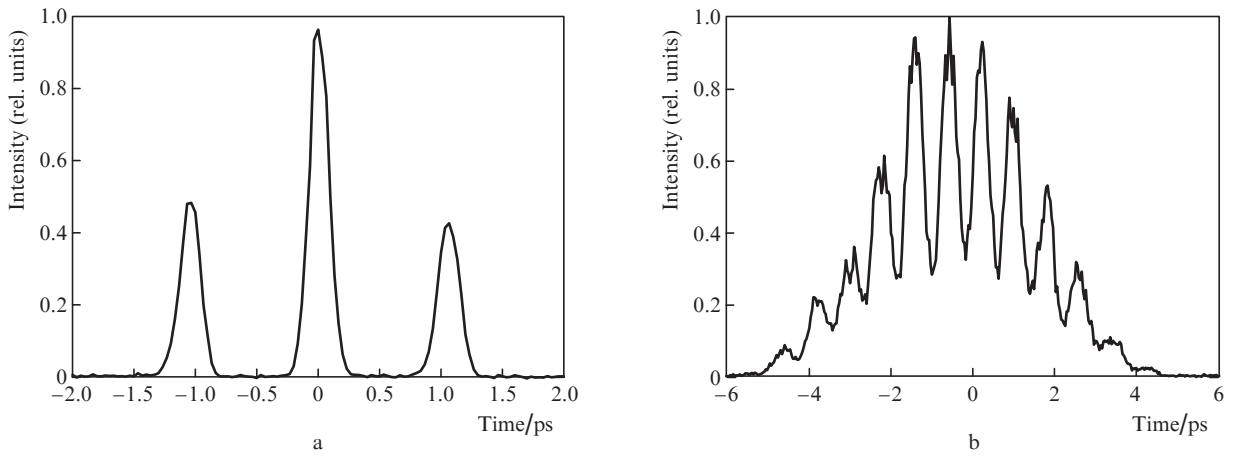

Figure 2. Autocorrelation function of (a) two transform-limited pulses having the duration $T_0 = 120$ fs and (b) two chirped pulses having the duration $T_1 = 2.2$ ps. The time delay between the pulses is $\tau = 1.1$ ps.

was measured using the autocorrelator in the noncollinear geometry. When the delay between the pulses increases, the period of chirped pulses modulation decreases and the number of maxima grows.

The THz emission spectrum was reconstructed form the first-order correlation function measured using the autocorrelator, assembled according to the Michelson interferometer scheme [25], in which an optoacoustic transducer (the Golay cell) played the role of a detector. The THz radiation was focused on the input window of the Golay cell by means of an off-axis parabolic mirror with the effective focal length 76 mm. To suppress the pump radiation at the wavelength 1230 nm and the second-harmonic radiation at the wavelength 615 nm, generated in the OH1 crystal, we used a special filter that transmitted only the radiation with the wavelength above 25 μm. The measurement of the THz radiation autocorrelation functions was performed in the chamber with dried air (the relative air humidity not exceeding 2%) to minimise the spectrum distortions due to the strong absorption of THz radiation by water vapours.

As mentioned above, the generation of THz pulses with a narrow spectrum can be obtained using the method of mixing of two linearly chirped pulses with a delay between them in a nonlinear medium. In this case, the centre frequency f_0 and the spectral width Δf of the generated THz radiation are determined by the expressions [26]:

$$f_0 = \frac{\tau}{\pi T_1 T_0}, \tag{3}$$

$$\Delta f = \frac{\sqrt{8}}{2\pi T_1}. \tag{4}$$

The maximal possible duration of a chirped pulse, measured in the experiments using AODDLs, was equal to 2.2 ps, while the minimal expected radiation spectral width, according to Eqn (4), equals ~0.2 THz. Note, that for an additional increase in the laser pulse duration and, therefore, narrowing the spectrum of THz radiation, one can use mechanical tuning of the compressor in the laser system. However, the subject of the present paper was the electronic control of the radiation spectrum using exclusively the AODDL.

The restored spectrum of a single-period THz radiation pulse, generated in the OH1 crystal pumped by the radiation of the femtosecond Cr:forsterite laser, is presented in Fig. 3. From the spectral width, it is possible to determine the range of time delays τ between the two chirped pulses, necessary for tuning the frequency of radiation in the spectral range 0.5–2.5 THz. In correspondence with expression (3), the range of time delays between two chirped pulses lies in the interval 0.5–1.5 ps.

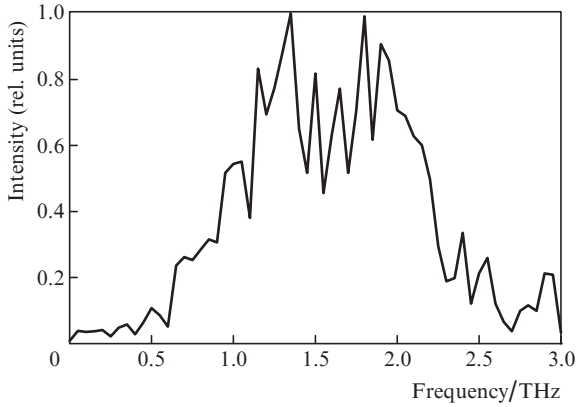

Figure 3. Spectrum of THz radiation at the output of the crystal OH1.

To obtain a maximal THz radiation pulse energy with a maximal conversion efficiency, it is necessary to provide the pump laser pulse energy density of ~10 mJ cm^{-2} [21] at the crystal.

In the experiments, we used the OH1 crystal having the diameter 4 mm, so that the energy of the laser pulse incident on the crystal had to be ~1.3 mJ. To provide the required energy value, the pulse energy at the output of the laser system was first reduced to 5 mJ by changing the delay time between the pump pulse output from multipass amplifiers and the amplified pulses at the radiation wavelength 1230 nm. Then, the energy was continuously controlled by means of the polarisation attenuator, consisting of a half-wave plate and a Glan–Thomson prism. The matching of the diameters of the laser beam and the OH1 crystal was implemented using a telescope.

3. Experimental results

In the experiments on generation of pulsed THz radiation with different centre frequencies, we used laser pulses with the temporal shape corresponding to the time delays of 0.5, 1 and 1.5 ps between two chirped pulses, each having the duration 2.2 ps.

From the measured autocorrelation functions of the THz pulses, we reconstructed the spectra, shown in Fig. 4. It is seen that the central part of the THz pulse is shifted depending on the delay between the laser pulses, and the spectral width amounts to ~0.25 THz. The energy of the THz pulses was measured using a SPI-D pyroelectric detector (Spectrum Detector Inc.) and amounted to 1.3, 6.2 and 1.7 μJ at the frequencies 0.6, 1.2 and 1.8 THz, respectively.

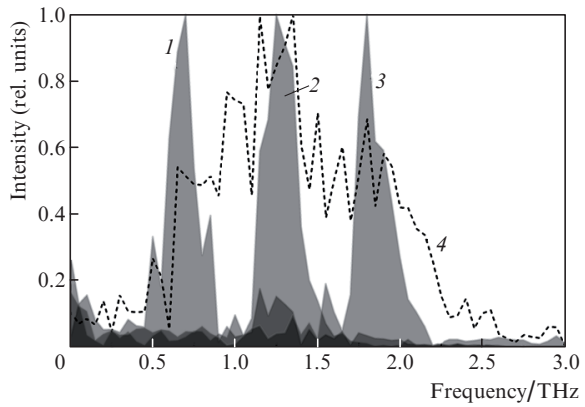

Figure 4. Spectra of THz radiation under pumping of the OH1 crystal with laser pulses of different temporal shape and the delay between two chirped pulses (*1*) 0.5, (*2*) 1 and (*3*) 1.5 ps; (*4*) is the spectrum in the case of pumping with a single transform-limited pulse.

4. Conclusions

We have experimentally demonstrated for the first time the generation of multi-period narrow-band THz pulses with different centre frequencies, using the method of optical rectification of profiled laser pulses from the Cr:forsterite laser system in the nonlinear organic crystal OH1. The adaptive tuning of the generation centre frequency occurs due to the formation of the appropriate multi-peak temporal profile of the laser pump pulse at the wavelength 1230 nm. For the first time the laser pulse formation of the necessary shape was implemented using the optical dispersion delay line, which allowed adaptive variation of the time delay between two chirped pulses and, therefore, the variation of the centre frequency of the generated terahertz pulses, as well as the control of their spectral width by changing the duration of the chirped pumping pulse.

We obtained the generation of THz pulses having the spectral width 250 GHz in the frequency range 0.5–2 THz and the energy from 1 to 6 μJ. An advantage of the method is the possibility of compensating for the reduction of the laser pulse energy after the diffraction in the acoustooptical dispersion delay line in the amplifier units of the laser system, operating in the saturation regime. The proposed method allows the adaptive control of the frequency and spectral width of the generated THz pulses almost in real time.

Note that the use of the present method for the formation of the multi-peak oscillation regime of the laser system requires careful adjustment of the gain, since in the scheme of the chirped pulse amplification, instead of a single pulse stretched in time, a sequence of shorter pulses can be amplified.

Acknowledgements. The experiments were performed using the unique terawatt femtosecond Cr:forsterite laser system developed at the Joint Institute for High Temperatures of the Russian Academy of Sciences. We also used the equipment of the Centre for Collective Use 'Laser Femtosecond Complex' of the Joint Institute for High Temperatures of the Russian Academy of Sciences.

The acoustooptical dispersion delay line was developed at the Acoustooptics Centre of Science, Technology and Education of the National University of Science and Technology MISiS under the support from Project 278 executed within the frameworks of the State Task in the Field of Research Activity No. 2014/113.

The work was supported by the Ministry of Education and Science of the Russian Federation (Agreement No. 14.613.21.0056, RFMEFI61316X0056) and by the National Science Foundation of Switzerland (Project IZLRZ2_164051).

References

1. Yeh K.-L., Hoffmann M.C., Hebling J., Nelson Keith A. *Appl. Phys. Lett*., **90** (3), 177721 (2007).
2. Hirori H., Doi A., Blanchard F., Tanaka K. *Appl. Phys. Lett*., **98** (3), 091106 (2011).
3. Huang S.W., Granados E., Huang W.R., Hong K.H., Zapata L.E., Kaertner F.X. *Opt. Lett*., **38** (5), 796 (2013).
4. Juranić P.N., Stepanov A., Ischebeck R., Schlott V., Pradervand C., Patthey L., Radović M., Gorgisyan I., Rivkin L., Hauri C.P., Monoszlai B., Ivanov R., Peier P., Liu J., Togashi T., Owada S., Ogawa K., Katayama T., Yabashi M., Abela R. *Opt. Express*, **22** (24), 30004 (2014).
5. Hochstrasser D.J., Cook R.M. *Opt. Lett*., **25** (16), 1210 (2000).
6. Daranciang D., Goodfellow J., Fuchs M., Wen H., Ghimire Sh., Reis D.A., Loos H., Fisher A.S., Lindenberg A.M. *Appl. Phys. Lett*., **99**, 141117 (2011).
7. Nahata A., Weling A.S., Heinz T.F. *Appl. Phys. Lett*., **69**, 2321 (1996).
8. Blanchard F., Razzari L., Bandulet H., et al. *Opt. Express*, **15** (20), 13212 (2007).
9. Hoffmann M.C., Yeh Ka-Lo, Hebling J., Nelson K.A. *Opt. Express*, **15** (18), 11706 (2007).
10. Fabian Brunner D.J., Lee S.-H., Kwon O., Feurer T. *Opt. Mater. Express*, **4** (8), 1587 (2014).
11. Vicario C., Ovchinnikov A.V., Ashitkov S.I., et al. *Opt. Lett*., **39** (23), 6632 (2014).
12. Krause J., Wagner M., Winnerl S., et al. *Opt. Express*, **19** (20), 19114 (2011).
13. Chen Z., Zhou X., Werley C.A., Nelson K.A. *Appl. Phys. Lett*., **99** (3), 071102 (2011).
14. Lu J., Hwang H.Y., Li X., Lee S.-H., et al. *Opt. Express*, **23** (17), 22723 (2015).
15. Avestisyan Y., Zhang C., Kawayama I., et al. *Opt. Express*, **20** (23), 25752 (2012).
16. Zhang C., Avetisyan Y., Abgaryan G., Kawayama I., Murakami H., Tonouchi M. *Opt. Lett*., **38** (6), 953 (2013).
17. Ahn J., Efimov A.V., Averitt R.D., Taylor A.J. *Opt. Express*, **11** (20), 2486 (2003).
18. Molchanov V.Ya., Chizhikov S.I., Makarov O.Yu., Solodovnikov N.P., Ginzburg V.N., Katin E.V., Khazanov E.A., Lozhkarev V.V., Yakovlev I.V. *Appl. Opt*., **48** (7), 118 (2009).
19. Molchanov V.Ya., Yushkov K.B. *Opt. Express*, **22** (13), 15668 (2014).

20. Molchanov V.Ya., Kitayev Yu.I., Kolesnikov A.I., Narver V.N., Rozenshteyn A.Z., Solodovnikov N.P., Shapovalenko K.G. *Teoriya i praktika sovremennoy akustiki* (Theory and Practice of Modern Acoustooptics) (Moscow: MISiS Publishing House, 2015).
21. Vicario C., Jazbinsek M., Ovchinnikov A.V., Chefonov O.V., Ashitkov S.I., Agranat M.B., Hauri C.P. *Opt. Express*, **23** (4), 4573 (2015).
22. Agranat M.B., Ashitkov S.I., Ivanov A.A., Konyashchenko A.V., Ovchinnikov A.V., Fortov V.E. *Kvantovaya Elektron*., **34** (6), 506 (2004) [*Quantum Electron*., **34** (6), 506 (2004)].
23. Molchanov V.Ya., Voloshinov V.B., Makarov O.Yu. *Kvantovaya Elektron*., **39** (4), 353 (2009) [*Quantum Electron*., **39** (4), 353 (2009)].
24. Chizhikov S.I., Garanin S.G., Goryachev L.V., Molchanov V.Ya., Romanov V.V., Rukavishnikov N.N., Sokolovskii S.V., Voronich I.N., Yushkov K.B. *Laser Phys. Lett*., **10** (1), 015301 (2013).
25. Lee Yun-Shik, Hurlbut W.C., Vodopyanov K.L., Fejer M.M., Kozlov V.G. *Appl. Phys. Lett*., **89** (3), 181104 (2006).
26. Weling A.S., Auston D.H. *J. Opt. Soc. Am. B*, **13** (12), 2783 (1996).